



Canadian Journal of Forest Research
Revue canadienne de recherche forestière

Fuel-related fire behaviour relationships for mixed live and dead fuels burned in the laboratory

Journal:	<i>Canadian Journal of Forest Research</i>
Manuscript ID	cjfr-2016-0457.R2
Manuscript Type:	Article
Date Submitted by the Author:	06-Apr-2017
Complete List of Authors:	Rossa, Carlos; UTAD, CITAB Fernandes, Paulo; Universidade de Trás-os-Montes e Alto Douro
Keyword:	fuel moisture content, spread rate, flame geometry, fuel consumption, wind-driven spread
Please Select from this Special Issues list if applicable:	N/A



Fire behaviour relationships for mixed fuels

Can. J. For. Res.

1 **Fuel-related fire behaviour relationships for mixed live and dead fuels burned**
2 **in the laboratory**

3 Carlos G. Rossa, and Paulo M. Fernandes

4

5

6 **C.G. Rossa, and P.M. Fernandes.** Centre for the Research and Technology of Agro-Environmental and Biological
7 Sciences (CITAB), University of Trás-os-Montes e Alto Douro (UTAD), Apartado 1013, 5001-801 Vila Real,
8 Portugal.

9 **Corresponding author:** Carlos G. Rossa (e-mail: carlos.g.rossa@gmail.com).

Draft

10 **Abstract:** A laboratory experimental program addressing fire spread in fuel beds composed of
11 dead foliage litter and vertically placed quasi-live branches, representative of many natural fuel
12 complexes, was carried out for either still air or wind conditions. Fuel bed characteristics, fire
13 spread rate, flame geometry and fuel consumption were assessed and empirical models for
14 estimating several parameters were developed. Weighted fuel moisture content (18–163%)
15 provided good estimates of fire behaviour characteristics and accounted for most of the variation
16 in still air and wind-driven spread rate ($0.1\text{--}1.3\text{ m min}^{-1}$). When predicting still-air fire spread rate,
17 fuel height was the most relevant fuel bed structural parameter and fuel type had significant
18 influence, whereas for wind-driven spread the effect of foliar fuel bed density was dominant and
19 fuel type became irrelevant. Flame length ($0.4\text{--}2.2\text{ m}$) increased from still air to wind-assisted (8
20 km h^{-1}) fire spread but its height remained constant. The fraction of total fuel load and mean
21 woody diameter consumed by fire were reasonably predicted from weighted fuel moisture content
22 alone, but predictions for the latter variable improved substantially by adding foliar fuel load.
23
24 *Key words:* fuel moisture content, spread rate, flame geometry, fuel consumption.

25 Introduction

26 A century has passed after the first attempts at predicting forest fire behaviour. The models that
27 have been developed since followed a wide variety of approaches, whose nature varied from
28 purely empirical to a virtually complete physical description of the mechanisms of fire spread
29 (Pastor 2003; Sullivan 2009). Spread rate (R_p) is the parameter most frequently sought to be
30 estimated, for which fuel moisture content (M) has been recognized as a critical factor very early
31 on (Show 1919).

32 The effect of dead fuel moisture content (M_d) on R_p is well established, but the same does not
33 apply to live fuel moisture content (M_l). In fact, evidence from field fires hints at no influence of
34 M_l on R_p (Alexander and Cruz 2013) or indicates a relatively weak and not entirely
35 consubstantiated effect (Anderson et al. 2015). This contrasts with theoretical formulations (e.g.,
36 Rothermel 1972; Van Wagner 1989) and results from laboratory experiments (Plucinski et al.
37 2010; Marino et al. 2012; Weise et al. 2016). Recently, laboratory fire-spread experiments in
38 quasi-live fuel beds, i.e., comprised of live plants when collected and whose M_l (13–180%) varied
39 as a function of storage time, showed a significant M_l effect on R_p , albeit low (Rossa et al. 2016).
40 However, the individual roles of M_d and M_l for fires spreading in mixtures of dead and live fuels
41 remain to be quantified. Fire-spread moisture damping is expected to differ between dead and live
42 fuel because differences in other fuel properties influence heat transfer and affect the ease with
43 which moisture can be evaporated (Wilson 1990; Catchpole and Catchpole 1991).

44 Research needs on the influence of fuel bed properties on fire behaviour in mixtures of dead
45 and live fuels go beyond the effect of M alone and extend to fuel bed structure as described by its
46 load (w), height (h), and bulk density (ρ). Empirical field studies invariably report the difficulties
47 in identifying and separating the effects of individual fuel properties on fire behaviour (Vega et al.

1998; Fernandes et al. 2000; Anderson et al. 2015). Obvious reasons for this are the natural heterogeneity in fuel complex properties, difficult to describe and to account for, and the existence of correlations between fuel descriptors, which complicates the detection and isolation of specific effects. Live fuel complexes have vertical orientation and are often tall and characterized by heavy fuel load, and for these reasons are difficult to be reproduced in the laboratory, having discouraged researchers from doing so. Weise et al. (2016) carried out an extensive set of laboratory fire spread experiments in shrub fuels, reported as ‘high-density’ and apparently not vertically oriented as in the field. Nelson and Adkins (1986) performed laboratory experiments of wind-driven fire spread in fuel beds of pine needles, over layered by vertical saw palmetto fronds, but fuel bed structure was maintained constant hindering the analysis of its effect on R_p . There is a great need for improved knowledge on the mechanisms of fire spread in live vegetation (Finney et al. 2013), because many fuel complexes are typically composed of live and dead fuels. Until those mechanisms are clearly established the task of predicting fire behaviour in natural fuel beds is greatly impaired.

We carried out a laboratory experimental burning program in mixed live and dead fuels, either in still air or wind conditions. The purpose was to increase understanding of the separate role of M_d and M_l on fire behaviour and to analyse the influence of relevant fuel structure descriptors such as h , w , and ρ . Spread rate, flame geometry and fuel consumption were measured and their variation described through empirical models.

Methods

Burn program

70 A total of 102 fire spread experiments in fuel beds composed of a litter layer (dead foliage) over
71 layered by vertically oriented quasi-live fuels, thus approaching the natural fuel structure, were
72 conducted in the University of Trás-os-Montes e Alto Douro (Vila Real, Portugal) between June
73 2015 and April 2016. All burn experiments were carried out on level ground, of which half under
74 still air conditions and half at 8-km h⁻¹ wind speed (U). Wind was measured in the absence of fire
75 just above the center of the fuel bed area, and resulted from a laminar flow induced by a 2.2 kW
76 ventilator (Soler & Palau Model CVTT-15/15). The experiments were time consuming, averaging
77 4–5 h per test, between fuel collection and preparation, building the fuel beds, and burning.

78

79 **Fuel species, collection, and storage**

80 The branches were obtained from two of the most abundant tree species in the Portuguese
81 forest, respectively *Eucalyptus globulus* Labill. (blue gum) and *Pinus pinaster* Ait. (maritime
82 pine). We collected one species at a time from a single location by cutting down ~5-year-old *P.*
83 *pinaster* and ~10-year-old *E. globulus* trees, removing the branches from the trunk, and carrying
84 them to the laboratory, where they were cut at 0.4 m and allowed to dry under ambient conditions
85 for a variable amount of time in order to get a wide range of moisture contents. M_l in this work
86 refers to quasi-live foliar moisture only and was measured independently from woody fuel
87 moisture content (M_{wd}). The former was periodically monitored using a fuel moisture analyzer
88 (Rossa et al. 2015) so that the experiments could be carried out over a well-distributed and wide
89 M_l range. We used foliar litter from *P. pinaster*, *E. globulus*, and *Pinus resinosa* Ait. (red pine).
90 Litter M_d is dependent on ambient conditions only, thus control of storage time was not a concern.

91

92 **Test rig, fuel bed preparation, and pre-burn sampling**

93 We used a 4-m long and 3.5-m wide combustion table uniformly covered with lightweight
94 expanded clay aggregate particles (LECA), allowing upright stem insertion. Fuel beds were 1-m
95 long and 1.2-m wide (Fig. 1). Three fuel complexes were used: *P. resinosa* litter with quasi-live *P.*
96 *pinaster* canopy (PR), *P. pinaster* litter with quasi-live *P. pinaster* canopy (PP), and *E. globulus*
97 litter with quasi-live *E. globulus* canopy (EG). The peculiar fuel combination used in the PR
98 experiments was an attempt to obtain fuel beds with a thin litter layer since *P. resinosa* litter is
99 more compact than *P. pinaster* litter. We carried out 24 PR tests but then proceeded with using *P.*
100 *pinaster* only as it was difficult to acquire the required quantity of *P. resinosa* needles.

101 *Fig. 1 about here*

102 We used five nominal levels of litter load, respectively 0.3, 0.5, 0.7, 0.9, and 1.1 kg m⁻², mostly
103 regularly distributed among the fuel type - wind mode combinations (Table 1). Litter load
104 measurement on a wet basis was adopted to avoid computing the M_d -corrected fuel weight. Actual
105 litter load (w_d) was calculated on a dry basis after measuring M_d . Branch load was not set to
106 specific levels. The first test of the day was usually used for determining a weight that would allow
107 a continuous canopy, and it was kept constant throughout the day. Nevertheless, the need for
108 managing the available branches, whose collection and preparation was the most time consuming
109 task, occasionally led to significant differences in the amount of fuel used in the experiments.
110 Because quasi-live fuel load (w_l) considered just the foliar component, the foliar fraction of *P.*
111 *pinaster* and *E. globulus* branches was estimated as the mean of 20 observations per species; each
112 was obtained by randomly selecting a branch from the fuel pile, removing its foliage, and
113 weighing the foliar and woody components. Fuel beds were prepared by spreading the litter fuel
114 first, and vertically inserting the branches afterwards, attaining homogeneous horizontal
115 distribution and vertical continuity with the litter layer (see Fig. 1).

116 *Table 1 about here*

117 Litter depth and distance from litter surface to the top of the fuel bed were measured ($n = 5$ for
 118 each), respectively before and after stem insertion. The sum of their means yielded h . Prior to
 119 ignition, air temperature (T) and relative humidity (RH) were measured with a pocket weather
 120 station. We collected three fuel samples to determine M_d (litter), M_l (quasi-live foliage) and M_{wd}
 121 (quasi-live woody fuel) by oven-drying at 105 °C during 24 h. Each sample comprised material
 122 collected from various locations in the fuel bed and cut into small pieces for faster and thorough
 123 drying. Using M_d , M_l , and the fractions of dead (f_d) and quasi-live (f_l) foliage, we computed the
 124 weighted foliar fuel moisture content (M_w):

$$125 \quad (1) \quad M_w = f_d \cdot M_d + f_l \cdot M_l$$

126 where quantities f_d and f_l were calculated using eq. 2 with either w_d or w_l as the numerator, or using
 127 eq. 3 when one of the fractions was known:

$$128 \quad (2) \quad f_d = \frac{w_d}{w_l + w_d}$$

$$129 \quad (3) \quad f_d + f_l = 1$$

130 Eq. 2 denominator corresponds to w , which accounts for foliar fuels only. Thus, Eq. 1 is equal to
 131 the ratio between the water mass contained in the fuel bed foliage (dead and quasi-live) and the
 132 total foliar dry mass. We obtained ρ by computing the ratio w/h .

133

134 **Ignition, fire behaviour, and fuel consumption**

135 The burn area was preceded by a 10-cm wide and approximately 2-cm deep strip of *P. pinaster*
 136 litter for facilitating fire spread through the canopy from the beginning of the fuel bed. A line of
 137 fire was rapidly established by lighting up a wool thread soaked in a 6:4 gasoline to diesel mixture.

Fire behaviour relationships for mixed fuels

Can. J. For. Res.

138 R_p was determined by measuring the time the base of the flame took to travel the length between
139 two cotton strings placed above the litter, which broke almost immediately after flame contact.
140 The strings were placed 0.9 m apart, leaving 5 cm at both the beginning and the end of the fuel bed
141 to diminish border effects during measurement.

142 Flame geometry was assessed when fire reached the fuel-bed midway, by visually estimating
143 average flame height (H_f), measured from the base of the fuel bed with the assistance of a tape
144 measure, and angle (φ). We evaluated φ by visually dividing the 90° between the horizontal and
145 the unburned fuel in two 45° sections, and then each of them in three 15° intervals and
146 approximating the flame angle to the nearest value. Trigonometry was used to calculate flame
147 length (L_f). We computed the ratio h/H_f , which for no-wind fires spreading on level ground is the
148 same as h/L_f because $L_f \approx H_f$. Flames always develop above the fuel bed ($H_f > h$) in well-sustained
149 fires, which means that $h/H_f < 1$. L_f cannot directly be inferred from h/H_f when fire spread is wind-
150 driven. Nonetheless, estimating H_f from this non-dimensional ratio should provide some
151 independence from fuel bed structure, because w is the structural parameter with greater influence
152 on flame dimensions (Fernandes et al. 2009) and is highly correlated with h in natural fuel
153 complexes (Fernandes 2001).

154 Five measurements were taken of the mean terminal diameter of woody fuels (D_{wd}) after fire
155 extinction. Branch remnants were weighed and assumed to be virtually moist free due to heat
156 exposure. We did not assess the remnants moisture content but they appeared extremely dry when
157 collected. Fuel load consumption was estimated as 90% of the difference between total initial fuel
158 dry weight and the remaining fuel, to account for ash (Burrows 2001). The fraction of fuel
159 consumed by fire (f_{cs}) was determined as the ratio of fuel consumption to total initial load.

160

161 **Data analysis and modelling**

162 Fuel bed parameters h , w , and ρ were considered for R_p modelling. We analyzed their
163 distributions by computing mean values and standard deviations, and checked for normality with
164 the Shapiro–Wilk test ($P > 0.05$) or, when significance was below the threshold value, for
165 approximate normality by visually inspecting their histograms.

166 R_p was modelled separately for the still air (R_0) and wind-driven fire spread (R_U) datasets. We
167 examined the M effect on R_p both as an exponential decay (e.g., Wilson 1990; Anderson et al.
168 2015) and a power law function (e.g., Burrows 1999; Cheney et al. 2012), and examined whether
169 M_d , M_l or M_w provided the highest explanation (coefficient of determination, R^2) of the observed
170 variability. Fuel structure metrics were then examined for their ability to improve the best-fitting
171 M -based equation. All functions were fitted in their log-transformed form by least-squares, as
172 often is the case in empirical fire behaviour modelling (Marsden-Smedley and Catchpole 1995;
173 Cheney et al. 2012). The bias inherent to back-transformation was corrected according to
174 Snowdon (1991). Model selection for a given fire behaviour variable took into account its practical
175 use and the R^2 value.

176 The ratio h/H_f and fuel consumption were modelled from the M metric that best explained R_p .
177 We described h/H_f and D_{wd} using linear relationships and again tested which fuel structure
178 variables added to the M -based explanation. As f_{cs} varies in the 0–1 range it was modelled using a
179 generalized linear model (GLM), fitted through an iterative process by maximum likelihood
180 estimation with a logit link function.

181 The influence of fuel bed type was examined after accounting for the effects of M and fuel bed
182 structure. In joint analysis of still air and wind-driven trials the effect of wind mode was examined

Fire behaviour relationships for mixed fuels

Can. J. For. Res.

183 as a categorical variable. Residuals were checked for approximate normality by visually
184 inspecting their histograms, and independence from predicted values was evaluated by correlation
185 analysis. In models with more than one independent variable the existence of significant
186 correlations between them was also verified. Predictions were evaluated based on deviation
187 measures, respectively root mean square error (RMSE), mean absolute error (MAE), mean
188 absolute percentage error (MAPE), and mean bias error (MBE) (Willmott 1982).

189

190 **Results**

191 **Data ranges**

192 The pre-burn duration of quasi-live fuel storage varied from one to 43 days. We aimed at
193 maintaining M_l above 50%, the typical minimum value for Mediterranean shrubs (Viegas et al.
194 2001), but it was occasionally lower, ranging between 30 and 214% (Table 2). The drying rate of
195 woody fuels was similar to that of foliage because M_{wd} (33–215%) was always very similar to M_l .
196 M_d varied narrowly (10–22%) as a result of moderate variation in ambient air conditions inside the
197 laboratory. M_w varied nine fold as a result of variation in M_l and M_d . The mass of foliage in *P.*
198 *pinaster* and *E. globulus* branches was 74.8 and 74.2% of the total, respectively. Except for *h*,
199 substantial variation was obtained regarding fuel structure, with f_d , w , and ρ varying approximately
200 by factors of five, three, and three. Fuel variables were normally distributed according to the
201 Shapiro-Wilk test, except the R_0 -dataset w distribution, which from visual inspection of its
202 histogram we concluded to be approximately normally distributed.

203

Table 2 about here

204 Fire behaviour and fuel consumption

205 Table 3 gives the R^2 for the tested models and Table 4 displays the results for those selected for
206 further analysis, including the fitted coefficients (a , b , c) and evaluation metrics for each equation.
207 R_p was better related to M_l than to M_d , both under still air and wind conditions, probably because
208 of the much larger range of the former. However, it was M_w that accounted for more variability. A
209 power law described the effect of M_w on R_p better than an exponential function, with R^2 increasing
210 ~20% to 0.753 and 0.821, respectively for still air and wind-driven spread. M_w accounted for most
211 of R_p variation but fuel bed parameters offered further improvement, with h and ρ producing the
212 greatest increase in R^2 , respectively for R_0 (up to 0.814) and R_U (up to 0.885) (eqs. 1 and 2 in Table
213 4). Fuel bed type exerted a significant ($P < 0.0001$) effect on R_0 and increased the R^2 by 17%, with
214 EG>PP>PR. For the sake of generalization, we decided not to include this variable in the model
215 (Fig. 2). The quality of fit was confirmed by MAPE of 18% and 13%, respectively for R_0 and R_U .
216 Predicted R_0 and R_U as a function of M_w are given in Fig. 3, respectively for $h = 0.33 \text{ kg m}^{-3}$ and ρ
217 $= 4.4 \text{ kg m}^{-3}$, the experimental means. For comparison purposes, Fig. 3 also displays a model of
218 the same form of eqs. 1 and 2 in Table 4, without the effects of fuel structure descriptors, and fitted
219 to Rossa et al. (2016) data for slope-driven spread (R_s) in quasi-live woody fuel beds; in these
220 experiments slope angle was 20° and h was 0.50–0.55 m.

221 *Table 3 about here*

222 *Fig. 2 about here*

223 *Fig. 3 about here*

224 When predicting h/H_f from M_w , the addition of w as an independent variable produced a modest
225 R^2 increase (3.8%). The model retained M_w only (eq. 3 in Table 4) for the sake of parsimony,
226 resulting in good fit (Fig. 4) with a MAPE of 11%.

227 *Fig. 4 about here*

228 The GLM model for f_{cs} (eq. 4 in Table 4, Fig. 5) had a MAPE of 15% ($n = 88$). Residuals of the
229 model differed by wind mode ($P = 0.007$), showing a slight tendency for higher f_{cs} in the presence
230 of wind. Using M_w alone to predict D_{wd} explained 66.7% of the existing variability. Adding w to
231 the equation increased R^2 by 10%, which justified its inclusion as an independent variable (eq. 5 in
232 Table 4). Predicted *v.* observed values are displayed in Fig. 6 and a MAPE of 12% indicates good
233 performance.

234 *Fig. 5 about here*

235 *Fig. 6 about here*

236 *Table 4 about here*

237 Discussion

238 M_w was a good predictor of both R_0 and R_U in fuel beds that combined live and dead fuels in
239 distinct layers, accounting for most of the variation in the dependent variables. This suggests that,
240 at least for practical purposes, vegetation phenology is irrelevant to fire spread in the sense that the
241 R_p response to M does not differ between live and dead fuels. The power-function damping effect
242 of M_w was not affected by wind mode, being similar for R_0 ($b = -0.7$) and R_U ($b = -0.6$) (Fig. 3),
243 and resulting in a R_p response equal to that observed in fuel beds composed of a single vegetative
244 state, as in Rossa et al. (2016) (see Fig. 3). The weak damping effect at M_w above ~100% is
245 explained by the ratio between fuel heat content and the energy necessary for fuel ignition
246 variation with M (Rossa 2017). Marino et al. (2012) also found M_w to be a good predictor of R_U in
247 laboratory-built shrub-litter fuel beds; their M_w range precluded conclusions about the effect on R_p
248 at $M_w > 80\%$. It follows that fuel complexes increasingly dominated by live fuels will exhibit more
249 marked seasonal variation in fire behaviour if drought impacts M_w , which is consistent with

250 reports of M_1 thresholds for increased fire activity (e.g., Dennison and Moritz 2009). The ‘real
251 world’ performance of our $M_w^{-0.63}$ damping effect for wind-assisted tests could be examined using
252 experimental field data, for which the role of M_1 on R remains uncertain (e.g., Anderson et al.
253 2015).

254 The contribution of fuel bed metrics to improve the prediction of R_p was modest, first of all
255 because the M effect was the study main focus and fuel structure was much less variable than M_w .
256 Also, most tests were carried out with h , w , and ρ close to their mean values. In the R_0 dataset the
257 means and coefficients of variation were $h = 0.33$ m (8.8%), $w = 1.5$ kg m⁻² (16.5%), and $\rho = 4.4$
258 kg m⁻³ (18.8%). In the R_U dataset we obtained $h = 0.35$ m (7.4%), $w = 1.5$ kg m⁻² (20.3%), and $\rho =$
259 4.4 kg m⁻³ (19.0%). In the wind-driven fire spread experiments the fuel bed parameter with the
260 highest leverage was ρ . A decrease of R_U with ρ is well established, both in the laboratory and in
261 field studies. Our $\rho^{-0.49}$ effect is stronger than in Marino et al. (2012) ($\rho^{-0.21}$) and very similar to that
262 reported by Anderson et al. (2015) ($\rho^{-0.48}$).

263 As ρ is given by w/h , a proper evaluation of the individual and interacting influences of w and h
264 requires measuring R_U at variable w for fixed h levels and vice versa, using a wide range in both w
265 and h . Catchpole et al. (1998) have shown that R_U rises with decreased w (at constant h) and
266 increased porosity. Then, it can be speculated that the ρ influence might be explained by a
267 combination of two effects: (i) higher w enhances combustion intensity and flames are more
268 difficult to tilt, diminishing heat transfer; and (ii) higher h increases porosity and favours heat
269 transfer (Holdich 2002).

270 The h/H_f equation revealed an interesting trait of flame geometry: H_f remained fairly constant
271 when fire spread was wind-assisted, although L_f increased as expected. Further experimentation is
272 needed for verifying if this relation holds for other wind speeds. If further studies confirm that h/H_f

Fire behaviour relationships for mixed fuels

Can. J. For. Res.

273 can be reasonably predicted based on M_w alone, its estimation can be operationally useful. Both h
274 and H_f can be visually assessed in the field and used to obtain a gross estimate of M_w in fuel
275 complexes composed of live and dead fuels.

276 The ability to predict f_{cs} is also useful in fire management but has been neglected in shrub-
277 dominated fuel types (Fernandes and Loureiro 2013; Ottmar 2014). The purpose of many
278 prescribed fire operations is to reduce fuel load. Being able *a priori* to predict the degree of fuel
279 consumption is important for planning and evaluating hazard-reduction burns. Predicting f_{cs} from
280 fuel moisture alone is appealing, although the difficulty in estimating M_1 is a relevant concern.
281 Using M_w as a single independent variable was less effective when predicting D_{wd} , and adding w to
282 the equation increased accuracy. The improvement makes sense, as burning a larger amount of
283 fine fuels increases fireline intensity which in turn allows consuming a larger amount of coarse
284 woody fuels, as found by several studies (e.g., Hollis et al. 2011).

285

286 **Summary and conclusions**

287 We carried out an experimental burning program in the laboratory in fuel beds composed of
288 litter and vertically arranged quasi-live branches, representative of many natural fuel complexes,
289 under either no-wind or wind conditions. We measured fuel bed characteristics, fire spread rate,
290 flame geometry, and fuel consumption, and fitted empirical equations that describe the effects of
291 the relevant independent variables.

292 M_w -based models allowed effective prediction of fire behaviour characteristics and fuel
293 consumption. We found no support for a differential role of live and dead fuel moisture content in
294 fire spread. M_w accounted for most of the observed variation in R_p for both still air and wind-
295 driven spread, although in no-wind conditions h was the most relevant fuel structure variable,

Fire behaviour relationships for mixed fuels

Can. J. For. Res.

296 whereas the effect of ρ dominated wind-driven spread. H_f remained constant during wind-assisted
297 fire spread although L_f increased. Reasonable predictions of f_{cs} and D_{wd} were obtained by using M_w
298 alone, but adding w as an independent variable substantially improved D_{wd} estimates.

299 Fire behaviour studies dedicated to fuel complexes with a relevant live fuel component are
300 scarce. This study results offer increased understanding of how fuel characteristics affect fire
301 behaviour in mixed live-dead fuels and are useful to inform subsequent experimental efforts in
302 relation to fire behaviour modelling and fire danger rating. As live and dead fuels in this study
303 formed contiguous layers, future efforts could examine whether fuel-related fire behaviour
304 relationships change with alternative fuel arrangements.

305

306 **Acknowledgements**

307 This work was supported by Fundação para a Ciência e a Tecnologia under post-doctoral grant
308 SFRH/BPD/84770/2012 (financing programs POPH and FSE) to the first author, and financed by
309 FEDER – Fundo Europeu de Desenvolvimento Regional funds through the COMPETE 2020 –
310 Operacional Programme for Competitiveness and Internationalisation (POCI), and by Portuguese
311 funds through FCT – Fundação para a Ciência e a Tecnologia in the framework of project POCI-
312 01-0145-FEDER-016727 (PTDC/AAG-MAA/2656/2014). Délio Sousa assisted with the logistics
313 of the experiments. Fernando Frazão, José A. Silva and Rafael Figueiredo assisted in fuel
314 collection. Two anonymous reviewers contributed with valuable comments.

315

316 **References**

317 Alexander, M.E., and Cruz M.G. 2013. Assessing the effect of foliar moisture content on the
318 spread rate of crown fires. *Int. J. Wildland Fire* **22**: 415–427. doi:10.1071/WF12008

Fire behaviour relationships for mixed fuels

Can. J. For. Res.

- 319 Anderson, W.R, Cruz, M.G., Fernandes, P.M., McCaw, L., Vega, J.A., Bradstock, R., Fogarty, L.,
320 Gould, J., McCarthy, G., Marsden-Smedley, J.B., Matthews, S., Mattingley, G., Pearce, G., and
321 Van Wilgen, B. 2015. A generic, empirical-based model for predicting rate of fire spread in
322 shrublands. *Int. J. Wildland Fire* **24**: 443–460. doi:10.1071/WF14130
- 323 Burrows, N.D. 1999. Fire behaviour in jarrah forest fuels: 2. Field experiments. *CALM Science* **3**:
324 57-84.
- 325 Burrows, N.D. 2001. Flame residence times and rates of weight loss of eucalypt forest fuel
326 particles. *Int. J. Wildland Fire* **10**: 137–143. doi:10.1071/WF01005
- 327 Catchpole, E.A., and Catchpole, W.R. 1991. Modelling moisture damping for fire spread in a
328 mixture of live and dead fuels. *Int. J. Wildland Fire* **1**: 101–106.
- 329 Catchpole, W.R, Catchpole, E.A., Rothermel, R.C., Morris, G.A, Butler, B.W., and Latham, D.J.
330 1998. Rate of spread of freeburning fires in woody fuels in a wind tunnel. *Combust. Sci.*
331 *Technol.* **131**: 1–37. doi:10.1080/00102209808935753
- 332 Cheney, N.P., Gould, J.S., McCaw, W.L., and Anderson, W.R. 2012. Predicting fire behaviour in
333 dry eucalypt forest in southern Australia. *Forest Ecol. Manag.* **280**: 120–131.
334 doi:10.1016/J.FORECO.2012.06.012
- 335 Dennison, P.E., and Moritz, M.A. 2009. Critical live fuel moisture in chaparral ecosystems: a
336 threshold for fire activity and its relationship to antecedent precipitation. *Int. J. Wildland Fire*
337 **18**: 1021–1027. doi:10.1071/WF08055
- 338 Fernandes, P.M., Catchpole, W.R., and Rego, F.C. 2000. Shrubland fire behaviour modelling with
339 microplot data. *Can. J. For. Res.* **30**: 889–899. doi:10.1139/X00-012
- 340 Fernandes, P.M. 2001. Fire spread prediction in shrub fuels in Portugal. *Forest Ecol. Manag.* **144**:
341 67–74. doi:10.1016/S0378-1127(00)00363-7

Fire behaviour relationships for mixed fuels

Can. J. For. Res.

- 342 Fernandes, P.M., Botelho, H.S., Rego, F.C., and Loureiro, C. 2009. Empirical modelling of
343 surface fire behaviour in maritime pine stands. *Int. J. Wildland Fire* **18**: 698–710.
344 doi:10.1071/WF9930193
- 345 Fernandes, P.M., and Loureiro, C. 2013. Fine fuels consumption and CO₂ emissions from surface
346 fire experiments in maritime pine stands in northern Portugal. *For. Ecol. Manag.* **291**: 344-356.
347 doi:10.1016/j.foreco.2012.11.037
- 348 Finney, M.A., Cohen, J.D., McAllister, S.S., and Jolly, W.M. 2013. On the need for a theory of
349 wildland fire spread. *Int. J. Wildland Fire* **22**: 25–36. doi:10.1071/WF11117
- 350 Holdich, R.G. 2002. Particle technology. Midland Information Technology and Publishing, UK.
- 351 Hollis, J.J., Anderson, W.R., McCaw, W.L., Cruz, M.G., Burrows, N.D., Ward, B., Tolhurst, K.G.,
352 and Gould, J.S. 2011. The effect of fireline intensity on woody fuel consumption in southern
353 Australian eucalypt forest fires. *Aust. For.* **74**: 81-96. doi:10.1080/00049158.2011.10676350
- 354 Marino, E., Dupuy, J.L., Pimont, F., Guijarro M., Hernando, C., and Linn, R. 2012. Fuel bulk
355 density and fuel moisture content effects on fire rate of spread: a comparison between FIRETEC
356 model predictions and experimental results in shrub fuels. *J. Fire Sci.* **30**: 277–299.
357 doi:10.1177/0734904111434286
- 358 Marsden-Smedley JB, Catchpole WR (1995) Fire behaviour modelling in Tasmanian buttongrass
359 moorlands. II. Fire behaviour. *Int. J. Wildland Fire* **5**: 215–228. doi:10.1071/WF9950215
- 360 Nelson, R.M., and Adkins, C.W. 1986. Flame characteristics of wind-driven surface fires. *Can. J.*
361 *For. Res.* **16**: 1293–1300. doi:10.1139/X86-229
- 362 Ottmar, R.D. 2014. Wildland fire emissions, carbon, and climate: modeling fuel consumption. *For.*
363 *Ecol. Manag.* **317**: 41–50. doi:10.1016/j.foreco.2013.06.010

Fire behaviour relationships for mixed fuels

Can. J. For. Res.

- 364 Pastor, E., Zarate, L., Planas, E., and Arnaldos, J. 2003. Mathematical models and calculation
365 systems for the study of wildland fire behaviour. *Prog. Energ. Combust.* **29**: 139–153.
366 doi:10.1016/S0360-1285(03)00017-0
- 367 Plucinski, M.P., Anderson, W.R., Bradstock, R.A., and Gill, A.M. 2010. The initiation of fire
368 spread in shrubland fuels recreated in the laboratory. *Int. J. Wildland Fire* **19**: 512–520.
369 doi:10.1071/WF09038
- 370 Rossa, C.G., Fernandes, P.M., and Pinto, A. 2015. Measuring foliar moisture content with a
371 moisture analyzer. *Can. J. For. Res.* **45**: 776–781. doi:10.1139/CJFR-2014-0545
- 372 Rossa, C.G., Veloso, R., and Fernandes, P.M. 2016. A laboratory-based quantification of the effect
373 of live fuel moisture content on fire spread rate. *Int. J. Wildland Fire* **25**: 569–573.
374 doi:10.1071/WF15114
- 375 Rossa, C.G. 2017. The effect of fuel moisture content on the spread rate of forest fires in the
376 absence of wind or slope. *Int. J. Wildland Fire*. doi:10.1071/WF16049
- 377 Rothermel, R.C. 1972. A mathematical model for predicting fire spread in wildland fuels. USDA
378 For. Serv. Res. Pap. INT-115.
- 379 Show, S.B. 1919. Climate and forest fires in Northern California. *J. Forest.* **17**: 965–979.
- 380 Snowdon, P. 1991. A ratio estimator for bias correction in logarithmic regressions. *Can. J. For.*
381 *Res.* **21**: 720–724. doi:10.1139/X91-101
- 382 Sullivan, A.L. 2009. Wildland surface fire spread modelling; 1990-2007. 1: Physical and quasi-
383 physical models. *Int. J. Wildland Fire* **18**: 349-368. doi:10.1071/WF06143
- 384 Van Wagner, C.E. 1989. Prediction of crown fire behavior in conifer stands. *In* Proceedings of the
385 Tenth Conference on Fire and Forest Meteorology, 17 – 21 April 1989, Ottawa, Ont. *Edited by*
386 D.C. MacIver, H. Auld and R. Whitewood. pp. 207–212.

- 387 Vega, J.A., Cuiñas, P., Fontúrbel, T., Pérez-Gorostiaga, P., and Fernández, C. 1998. Predicting fire
388 behaviour in Galician (NW Spain) shrubland fuel complexes. *In* Proceedings of the 3rd
389 International Conference on Forest Fire Research and 14th Fire and Forest Meteorology
390 Conference, 16–20 Nov. 1998, Luso, Portugal. *Edited by* D.X. Viegas. Associação para o
391 Desenvolvimento da Aerodinâmica Industrial, University of Coimbra, Portugal. pp. 713–728.
- 392 Viegas, D.X., Piñol, J., Viegas, M.T., and Ogaya, R. 2001. Estimating live fine fuels moisture
393 content using meteorologically-based indices. *Int. J. Wildland Fire* **10**: 223–240.
394 doi:10.1071/WF01022
- 395 Weise, D.R., Koo, E., Zhou, X., Mahalingam, S., Morandini, F., and Balbi, J.H. 2016. Fire spread
396 in chaparral—a comparison of laboratory data and model predictions in burning live fuels. *Int. J.*
397 *Wildland Fire* **25**: 980-994. doi:10.1071/WF15177
- 398 Willmott, C.J. 1982. Some comments on the evaluation of model performance. *B. Am. Meteorol.*
399 *Soc.* **63**: 1309–1313. doi:10.1175/1520-0477(1982)063<1309:SCOTEO>2.0.CO;2.
- 400 Wilson, R.A. 1990. Reexamination of Rothermel's fire spread equations in no-wind and no-slope
401 conditions. USDA For. Serv. Res. Pap. INT-434.

402

403 **List of symbols**404 a, b, c , fitted coefficients used in several equations405 D_{wd} (mm), mean post-fire terminal diameter of woody fuels406 f_{cs} , fraction of the total fuel load consumed by fire (including woody components)407 f_d , fraction of dead fuels408 f_l , fraction of live or quasi-live fuels409 h (m), fuel bed height

Fire behaviour relationships for mixed fuels

Can. J. For. Res.

- 410 H_f (m), flame height (measured from the base of the fuel bed)
- 411 L_f (m), flame length (measured from the base of the fuel bed)
- 412 M (%), fuel moisture content (dry basis)
- 413 M_d (%), dead foliage moisture content
- 414 M_l (%), live or quasi-live foliage moisture content
- 415 M_w (%), weighted foliar fuel moisture content
- 416 M_{wd} (%), woody fuel moisture content
- 417 R_p (m min⁻¹), fire spread rate
- 418 R_s (m min⁻¹), slope-driven fire spread rate
- 419 R_U (m min⁻¹), wind-driven fire spread rate
- 420 R_0 (m min⁻¹), basic fire spread rate (i.e., on level ground in the absence of wind)
- 421 RH (%), air relative humidity
- 422 T (°C), air temperature
- 423 U (km h⁻¹), wind speed
- 424 w (kg m⁻²), total foliar fuel load (dry basis)
- 425 w_d (kg m⁻²), litter fuel load
- 426 w_l (kg m⁻²), live or quasi-live foliage fuel load
- 427
- 428 **Greek symbols**
- 429 ϕ (°), flame angle (measured between the flame and the unburned fuel bed)
- 430 ρ (kg m⁻³), foliar fuel bed density

Fire behaviour relationships for mixed fuels

Can. J. For. Res.

431 **Tables and table captions**432 **Note:** The tables below embedded as pictures were uploaded separately as individual files.

433

434 **Table1.** Nominal litter fuel load (wet-basis) repetitions per fuel bed and wind mode

Fuel load (kg m ⁻²)	PR		PP		EG	
	no-wind	wind	no-wind	wind	no-wind	wind
0.3	4	4	4	5	4	5
0.5	4	4	4	5	4	5
0.7	4	4	4	5	4	5
0.9	-	-	9	9	-	-
1.1	-	-	6	-	-	-

435

436 **Note:** PR, litter of dead *Pinus resinosa* needles and canopy of quasi-live *Pinus pinaster*437 branches; PP, litter of dead *P. pinaster* needles and canopy of quasi-live *P. pinaster* branches; EG,438 litter of dead *Eucalyptus globulus* leaves and canopy of quasi-live *E. globulus* branches.

Draft

439 **Table 2.** Range of main experimental parameters (see ‘List of symbols’ for an explanation of
 440 variables).

Fuel bed	U (km h ⁻¹)	n	h (m)	T (°C)	RH (%)	M_a (%)	M_l (%)	f_a	M_v (%)	w (kg m ⁻²)	ρ (kg m ⁻³)	R_p (m min ⁻¹)	ϕ (°)	L_t (m)	D_{wd} (mm)
PR	0	12	0.309–0.361	20.8–26.3	57.5–81.0	14.0–22.4	81.2–213.6	0.19–0.38	69.3–161.7	1.27–1.62	3.87–4.69	0.127–0.281	90	0.35–0.75	1.0–4.5
	8	12	0.292–0.380	20.8–26.3	57.5–81.0	14.8–19.4	74.8–221.1	0.20–0.39	59.1–163.0	1.24–1.65	3.91–4.85	0.143–0.540	45–75	0.37–0.92	2.0–4.2
PP	0	27	0.263–0.380	14.7–26.8	48.3–71.3	12.3–19.7	55.7–155.5	0.18–0.64	35.7–123.1	1.17–1.85	3.51–5.77	0.111–0.308	90	0.40–0.95	2.6–6.3
	8	24	0.305–0.374	14.7–26.8	47.5–71.3	12.7–21.6	47.1–158.7	0.18–0.47	34.3–124.0	1.14–1.92	3.57–5.88	0.249–0.666	45–60	0.57–1.27	2.6–5.8
EG	0	12	0.336–0.398	20.4–23.5	43.7–73.0	10.0–14.8	30.3–90.9	0.20–0.62	21.1–66.5	0.67–1.69	1.98–4.34	0.199–0.656	90	0.60–1.20	3.5–6.2
	8	15	0.327–0.406	20.0–23.5	43.7–73.0	9.8–12.8	28.9–95.8	0.13–0.61	18.0–77.1	0.66–2.43	2.02–6.10	0.416–1.285	30–45	1.27–2.20	3.5–6.0

441
 442 **Note:** PR, litter of dead *Pinus resinosa* needles and canopy of quasi-live *Pinus pinaster*
 443 branches; PP, litter of dead *P. pinaster* needles and canopy of quasi-live *P. pinaster* branches; EG,
 444 litter of dead *Eucalyptus globulus* leaves and canopy of quasi-live *E. globulus* branches.

Draft

445 **Table 3.** Coefficient of determination R^2 for the tested models; for each variable the highest R^2 is
 446 shown in bold font (see ‘List of symbols’ for an explanation of variables).

Variable	Model	n	R^2
R_0	$a \exp(b M_d)$	51	0.067
	$a \exp(b M_i)$		0.641
	$a \exp(b M_w)$		0.647
	$a M_w^b$		0.753
	$a M_w^b h^c$		0.814
	$a M_w^b w^c$		0.770
	$a M_w^b \rho^c$		0.799
R_U	$a \exp(b M_d)$	51	0.143
	$a \exp(b M_i)$		0.655
	$a \exp(b M_w)$		0.665
	$a M_w^b$		0.821
	$a M_w^b h^c$		0.819
	$a M_w^b w^c$		0.881
	$a M_w^b \rho^c$		0.885
h/H_f	$a + b M_w$	102	0.833
	$a + b M_w + c h$		0.833
	$a + b M_w + c w$		0.865
	$a + b M_w + c \rho$		0.864
D_{wd}	$a + b M_w$	102	0.667
	$a + b M_w + c h$		0.676
	$a + b M_w + c w$		0.732
	$a + b M_w + c \rho$		0.712

447

Draft

Fire behaviour relationships for mixed fuels

Can. J. For. Res.

448 **Table 4.** Coefficients and evaluation metrics for the selected models; 95% confidence intervals for
 449 a , b and c are shown in parenthesis (see ‘List of symbols’ for an explanation of variables).

450

Model	a	b	c	RMSE	MAE	MAPE	MBE
[1] $R_0 = a M_w^b h^c$	12.657 (5.078–31.55)	-0.7443 (-0.8592– -0.6295)	0.8090 (0.1389–1.479)	0.0556	0.0432	17.7	0.00
[2] $R_U = a M_w^b \rho^c$	13.14 (8.035–21.50)	-0.6253 (-0.7212– -0.5293)	-0.4895 (-0.7335– -0.2456)	0.0723	0.0545	12.7	0.00
[3] $h/H_f = a + b M_w$	0.1998 (0.1687–0.2310)	0.00443 (0.004036–0.004823)	-	0.0689	0.0535	11.1	0.00
[4] $f_{cs} = 1 / (1 + \exp(-(a + b M_w)))$	2.647 (1.415–4.047)	-0.03064 (-0.04974– -0.01346)	-	0.0757	0.0586	14.9	0.00
[5] $D_{wd} = a + b M_w + c w$	4.316 (3.617–5.015)	-0.02553 (-0.02886– -0.02221)	1.041 (0.621–1.461)	0.5782	0.4441	12.2	0.00

Draft

451 **Figures and figure captions**452 **Note:** The figures below embedded as pictures were uploaded separately as individual files.

453

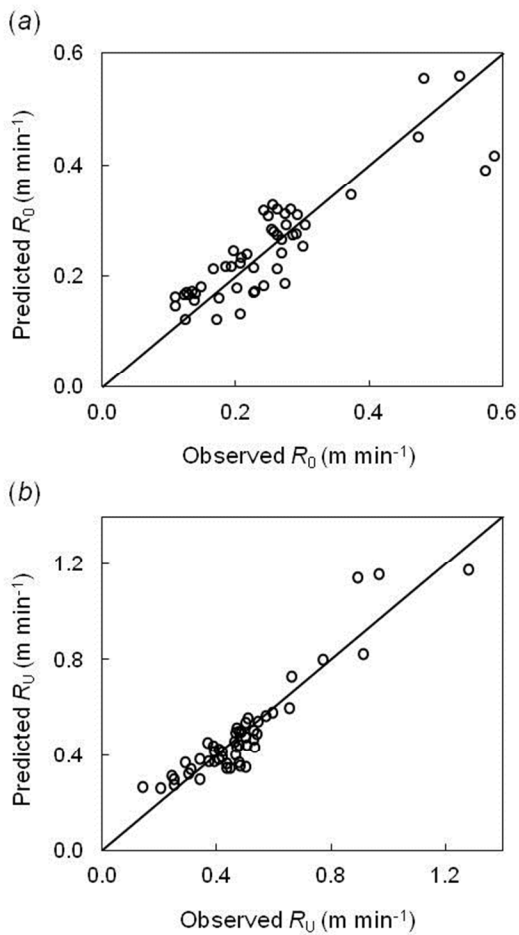
454 **Fig. 1.** Combustion table with a fuel bed of *Eucalyptus globulus* leaves litter over layered by455 quasi-live vertical *E. globulus* branches during a wind-driven (8 km h^{-1}) fire spread test.

456

Fire behaviour relationships for mixed fuels

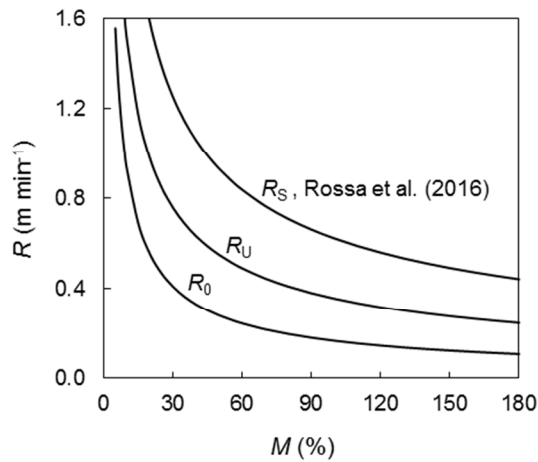
Can. J. For. Res.

457 **Fig. 2.** Predicted *v.* observed: (a) basic fire spread rate (R_0); (b) wind-driven fire spread rate (R_U , U
458 = 8 km h⁻¹). The solid lines correspond to perfect agreement. Model equations, coefficients, and
459 evaluation metrics are in Table 4.



460

461 **Fig. 3.** Predicted basic fire spread rate (R_0) for constant fuel bed height ($h = 0.33$ m, experimental
462 mean), wind-driven fire spread rate (R_U , $U = 8$ km h⁻¹) for constant foliar fuel bed density ($\rho = 4.4$
463 kg m⁻³, experimental mean), and slope-driven fire spread rate (laboratory data of 50 tests in fuel
464 beds of quasi-live vertical branches with a slope angle of 20° retrieved from Rossa et al. 2016, $R_s =$
465 $8.98 M^{-0.579}$, $R^2 = 0.667$), as a function of foliar fuel moisture content (M). Model equations,
466 coefficients, and evaluation metrics for R_0 and R_U are in Table 4.

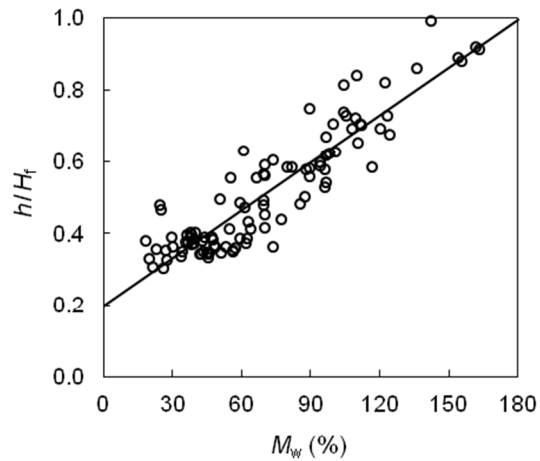


467

Fire behaviour relationships for mixed fuels

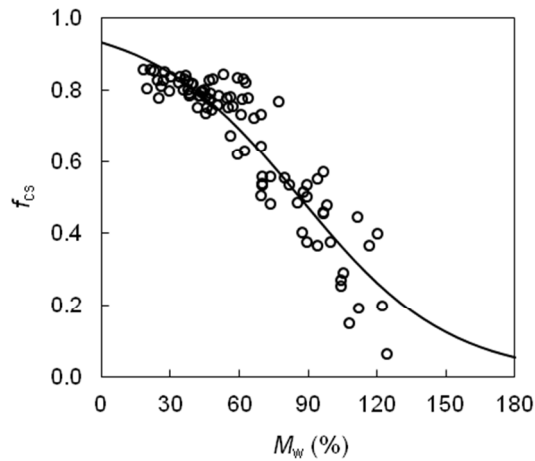
Can. J. For. Res.

468 **Fig. 4.** Ratio between fuel bed height (h) and flame height (H_f) (measured from the base of the fuel
469 bed) as a function of weighted foliar fuel moisture content (M_w). The solid line corresponds to the
470 model equation whose coefficients and evaluation metrics are in Table 4.



471

472 **Fig. 5.** Fraction of the total fuel load consumed by fire (f_{cs}) as a function of weighted foliar fuel
473 moisture content (M_w). The solid line corresponds to the model equation whose coefficients and
474 evaluation metrics are in Table 4.

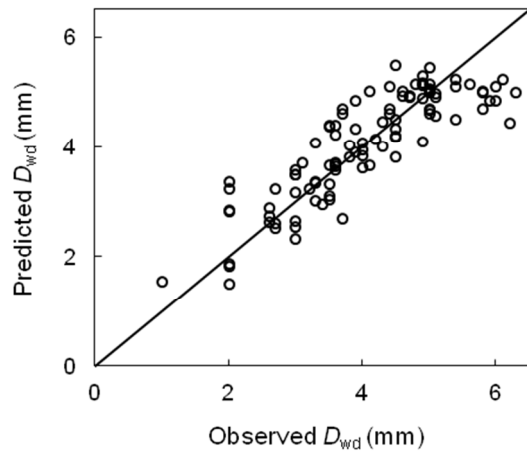


475

Fire behaviour relationships for mixed fuels

Can. J. For. Res.

476 **Fig. 6.** Predicted *v.* observed mean post-fire terminal diameter of woody fuels (D_{wd}). The solid line
477 corresponds to perfect agreement. Model equation, coefficients, and evaluation metrics are in
478 Table 4.



479